ELSEVIER

Chemical Engineering Journal 117 (2006) 253–261

Chemical Engineering Journal

www.elsevier.com/locate/cej

Removal of Cr^{3+} in fixed bed using zeolite NaY

F.C. Gazola [a], M.R. Pereira [a], M.A.S.D. Barros [a,*], E.A. Silva [b], P.A. Arroyo [a]

[a] *State University of Maringá, Chemical Engineering Department, Maringá-Brazil 5790 Colombo Av., Bl. D-90, 87020-900 Maringá, Brazil*
[b] *West Paraná State University, Chemical Engineering Department, 645 Faculdade St. 645, Jardim La Salle, 85903-000 Toledo, Brazil*

Received 28 January 2005; received in revised form 6 September 2005; accepted 14 November 2005

Abstract

In this work the chromium exchange mechanism in zeolite NaY was studied. The breakthrough data were determined in an up-flow fixed bed at 30 °C using three bed heights: 1.5, 3.0 and 4.5 cm. It was seen that the bed height influenced the maximum chromium uptake as well as the mass transfer zone due to changes in pH during the ion exchange process. Changes in pH generated different chromium species with particular difficulties in diffusing towards the exchange sites of the zeolite. The linear driving force (LDF) model for breakthrough curves fitted well to the experimental data and the estimated overall mass transfer coefficient also changed with bed height, which is a consequence of different chromium speciation in the ion exchange mechanism. The axial dispersion coefficient can be considered as an average of 8.25×10^2, 1.04×10^2 and 3.36×10^2 cm^2/min for the bed heights of 1.5, 3.0 and 4.5 cm, respectively.

Keywords: Zeolite; Chromium; Equilibrium data; Breakthrough curve

1. Introduction

Aquatic contamination by heavy metals is very harmful since these elements are not degradable in the environment and may accumulate in living organisms. One of the most important heavy metal is chromium. Chromium occurs in the workplace predominantly in two valence states: hexavalent chromium [Cr^{6+}] and trivalent chromium [Cr^{3+}] [1]. Hexavalent and trivalent chromium compounds find extensive application in diverse industries. Hexavalent chromium is very toxic and commonly related to cytotoxicity and carcinogenicity [2]. On the other hand, trivalent chromium is less toxic but can be easily oxidized to the hexavalent form in the last stages of industrial wastewater treatment [3]. Therefore, it is important to minimize the Cr^{3+} residue before its oxidation. There is a wide variety of techniques available for the Cr^{3+} recovery and the most widely used is precipitation with alkalis. Nevertheless, after filtration of the sludge, the liquid phase still contains trivalent chromium. Ion exchange is one of the most effective techniques for such liquid phases. Many ion exchangers or adsorbents for chromium removal have being studied, such as carbon [4,5], resins [1] and zeolites [6,7].

Zeolites are known as very good ion exchangers due to their high cation exchange capacity. Among them, zeolite Y is one of the most promising synthetic zeolites for environmental purposes because it has an open negatively charged framework where easily exchangeable balancing cations are located [8]. Moreover, when compared to other molecular sieves, zeolite NaY seems to be more selective to Cr^{3+} ions even than its isomorphic framework, zeolite NaX, that has higher cation exchange capacity (CEC) due to differences in the cation-framework interaction [9].

Most separation and purification processes that employ sorption technology use continuous-flow columns [10]. This operating mode ensures the highest possible concentration difference driving force and dispenses a subsequent solid–liquid separation process. In such systems mass-transfer resistances are important and the overall dynamics of the system determine the efficiency of the process, rather than just the equilibrium considerations [11].

Therefore, in order to effectively design zeolite-bearing materials units, the development of mathematical models that can successfully simulate the experimental breakthrough operation is required. These models should be able to predict the dynamics of the ion-exchange process in order to facilitate the development of novel applications such as NaY packed beds for chromium removal from wastewater. The LDF model assumed that driving

* Corresponding author. Fax: +55 44 223 3440.
E-mail address: angelica@deq.uem.br (M.A.S.D. Barros).

1385-8947/$ – see front matter © 2005 Elsevier B.V. All rights reserved.
doi:10.1016/j.cej.2005.11.014

Nomenclature

C	concentration of the chromium in the bulk fluid phase (mequiv./L)
CEC	cation exchange capacity (mequiv./g)
C_{eq}	equilibrium concentration of the chromium in the bulk fluid phase (mequiv./L)
C_0	initial concentration of the chromium in the bulk fluid phase (mequiv./L)
C^F	concentration of the chromium in the inlet in the column (mequiv./L)
C_{out}^{EXP}	experimental concentration of the Cr(III) in the outlet of the column (mequiv./L)
C_{out}^{MOD}	concentration of the Cr(III) determined by the solution of the model in the outlet of the column (mequiv./L)
D_L	axial dispersion coefficient (cm^2/min)
H	bed height (cm)
k_{rp}	Redlich–Peterson constant
K_S	overall mass transfer coefficient in the zeolite (min^{-1})
m_z	dry weight of the zeolite (g)
MTZ	length of mass transfer zone (cm)
np	number of experimental data points
q	concentration of chromium exchange in the zeolite (mequiv./g)
q_{eq}	equilibrium concentration of chromium exchange in the zeolite (mequiv./g)
$q_{max\text{-}eq}$	maximum equilibrium concentration of chromium exchange in the zeolite (mequiv./g)
$\dot{Q}$	volumetric flow rate (cm^3/min)
t	time (min)
t_t	saturation time (min)
t_u	break point time (min)
u	intersticial velocity (cm/min)
z	axial coordinate in the column (cm)
Z	bed height (cm)

Greek letters

α_{rp}	Redlich–Peterson constant
β	Redlich–Peterson constant
ε	column void fraction
ρ_b	fixed bed density (g/L)

Dimensionless group

Pe_b	Peclet number for the bed, Hu/D_L
St_D	Stanton number, $K_S u/H$
ξ	dimensionless axial coordinate, z/H
τ	dimensionless time coordinate, t_u/H

force for mass transfer to be linear with respect to the metal ion concentration in adsorbent and there are equilibrium in the fluid–solid interface [12]. Equilibrium isotherms were obtained through breakthrough data in order to perform equilibrium studies using columns [13]. Therefore, the mathematical model uses these dynamic isotherms, that means, isotherms obtained through breakthrough data. The model also predicts the axial dispersion coefficient in the bed. Therefore, this work aimed to study the mechanism of chromium uptake using zeolite NaY in a fixed bed. In order to achieve this purpose, breakthrough curves at three different bed heights (1.5, 3.0 and 4.5 cm) were investigated and the LDF model applied to the experimental data.

2. Experimental

2.1. Zeolite

The initial NaY zeolite was highly crystalline. NaY has the unit cell composition of $Na_{51}(AlO_2)_{51}(SiO_2)_{141}$ on a dry basis and a CEC of 3.90 mequiv./g. In order to obtain, as much as possible, the homoionic sodium form, the zeolite was mixed with 1 mol/L solution of NaCl four times at 60 °C at a proportion of 100 g of solid to 1 L of solution [14]. Then, each time the samples were washed with 2 L with hot deionized water and oven-dried at 100 °C. The pre-treated sample was pelletized, crushed and sieved with an average diameter of 0.180 mm previously recommended as the optimal particle size for this fixed-bed system [9].

2.2. Reagent

Reagent-grade $CrCl_3{\cdot}9H_2O$ was mixed with mixed deionized water to prepare chromium solutions from 0.27 to 2.10 mequiv./L at the pH range of 3–4.

2.3. Ion exchange unit

The column tests were carried out in a water-jacketed glass column at 30 °C with an inside diameter of 0.9 cm. The dried mass of zeolite pellets (m_z) of 0.33, 0.65 and 0.98 g filled the column generating the bed heights of 1.5, 3.0 and 4.5 cm, respectively. Deionized water was used to rinse the zeolite bed up flow in order to remove air bubbles. When the column was finally ready for the run, the flow rate was fixed to 9 cm^3/min as it was previously determined as the optimal flow rate for this system [9]. Runs were started by feeding the column with the chromium solution (C_0) also in up flow. In all dynamic tests the outlet samples (C) were regularly collected until the saturation of the bed ($C/C_0 = 1$) occurred and their concentration analyzed using a Varian atomic absorption spectrophotometer. Then, the breakthrough curves were plotted (C/C_0 versus t).

2.4. Dynamic ion exchange isotherms

The breakthrough data were used to calculate the amount of Cr^{3+} ions retained in each run through the mass balance. By such balance, it can be shown that the area of the curve $(1 - C/C_0)$ is proportional to the total solute retained. Therefore, the amount of Cr^{3+} ions retained in the zeolite-packed bed may be written

as:

$$q_{eq} = \frac{C_0 \dot{Q}}{1000 m_z} \int_0^\infty \left(1 - \frac{C}{C_0}\right) dt \quad (1)$$

where q_{eq} is the equilibrium concentration of chromium ions in the zeolite (mequiv./g), $\dot{Q}$ the solution flow rate (9 cm^3/min), C the outlet chromium concentration (mequiv./L), C_0 the feed concentration of chromium in the inlet column (mequiv./L), m_z the zeolite dry mass (g) and t is the running time (min).

The dynamic isotherm was plotted using q_{eq} versus C_0. Therefore, each breakthrough curve generated only one experimental point for the dynamic isotherm.

It must be emphasized that dynamic isotherms do not provide a true equilibrium as the contact time between fluid and solid phases is lower than the one obtained in a batch system. On the other hand "equilibrium" data obtained through breakthrough data can predict better the dynamic exchange [15].

2.5. The Redlich–Peterson model

The Redlich–Peterson model is given by

$$q_{eq} = \frac{k_{rp} C_0}{1 + \alpha_{rp} C_0^{\beta}} \quad (2)$$

where k_{rp}, α_{rp} and β are constants and $0 < \beta < 1$.

The experimental breakthrough data were fitted to the Redlich–Peterson model using the quasi-Newton regression presented in the software Statistica 6.0.

2.6. The mathematical model

In the model development the following hypotheses were considered:

- isobaric and isothermic process;
- constant porosity through the bed;
- constant horizontal cross-section of the bed;
- incompressible fluid and bed;
- fixed bed;
- constant flow rate through the bed;
- uniform flow rate across the bed cross-section;
- superficial adsorption;
- negligible radial dispersion.

The mathematical model for exchange of a metal ion in a fixed bed column was obtained by means of the mass balance equations applied to an element of volume of the column in the liquid phase and in the solid phase [15].

The mass balance equation for the fluid phase is

$$\frac{\partial C}{\partial \tau} + \rho_b \frac{1}{\varepsilon} \frac{\partial q}{\partial \tau} = -u \frac{\partial C}{\partial \xi} + \frac{1}{Pe_b} \frac{\partial^2 C}{\partial \xi^2} \quad (3)$$

with the following initial and boundary conditions:

$$C(\xi, 0) = C_0 \quad (4)$$

$$\frac{\partial C}{\partial \xi} = Pe_b (C(\tau, 0) - C^F) \text{ in } \xi = 0 \quad (5)$$

$$\frac{\partial C}{\partial \xi} = 0 \text{ in } \xi = 1 \quad (6)$$

Moreover, the mathematical model is based on the assumption that the exchange reaction is relatively fast, due to the very favorable shape of the Cr–NaY isotherms [6], and the migration in the adsorbent pores plays a dominant role in the process [16].

The mass transfer for ion diffusion in the adsorbent is represented by Fick's second law that is relatively complex. To facilitate the resolution of these systems of differential equations it is recommended to replace the Fick's law to a simplified kinetic expression [12].

In order to model the chromium exchange rate in the adsorbent it is assumed that the driving force for the mass transfer is linear with the concentration for solid phase, thus the exchange rate is represented by the following equation:

$$\frac{\partial q}{\partial \tau} = -St_D (q - q_{eq}) \quad (7)$$

with the following initial condition:

$$q(\xi, 0) = q_0 \quad (8)$$

The equilibrium concentration of chromium uptake in the adsorbent in mequiv./g (q_{eq}) was estimated by Redlich–Peterson isotherm model, already discussed.

To solve the system of partial equations together with the initial and boundary conditions and equilibrium relation, the domain of the problem was discretized in (np) elements. This

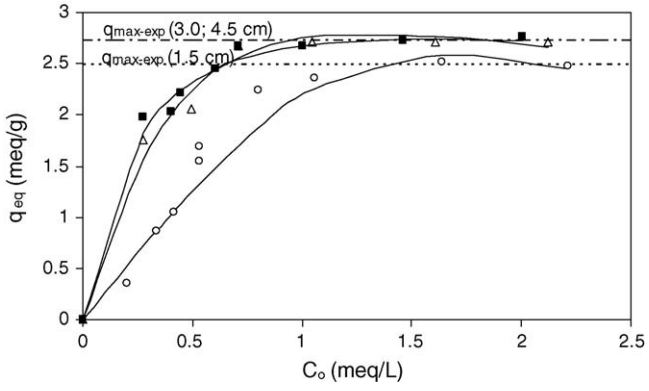

Fig. 1. Isotherms for different bed heights fitted to Redlich–Peterson model: (◯) $H = 1.5$ cm; (■) $H = 3.0$ cm; (△) $H = 4.5$ cm.

Table 1
Redlich–Peterson model for the three bed heights

Bed height (cm)	Redlich–Peterson isotherm	R^2
1.5	$q_{eq} = \frac{2.596 C_0}{1+0.192 C_0^{2.454}}$	0.988
3.0	$q_{eq} = \frac{10.999 C_0}{1+3.110 C_0^{1.189}}$	0.995
4.5	$q_{eq} = \frac{6.995 C_0}{1+1.546 C_0^{1.442}}$	0.994

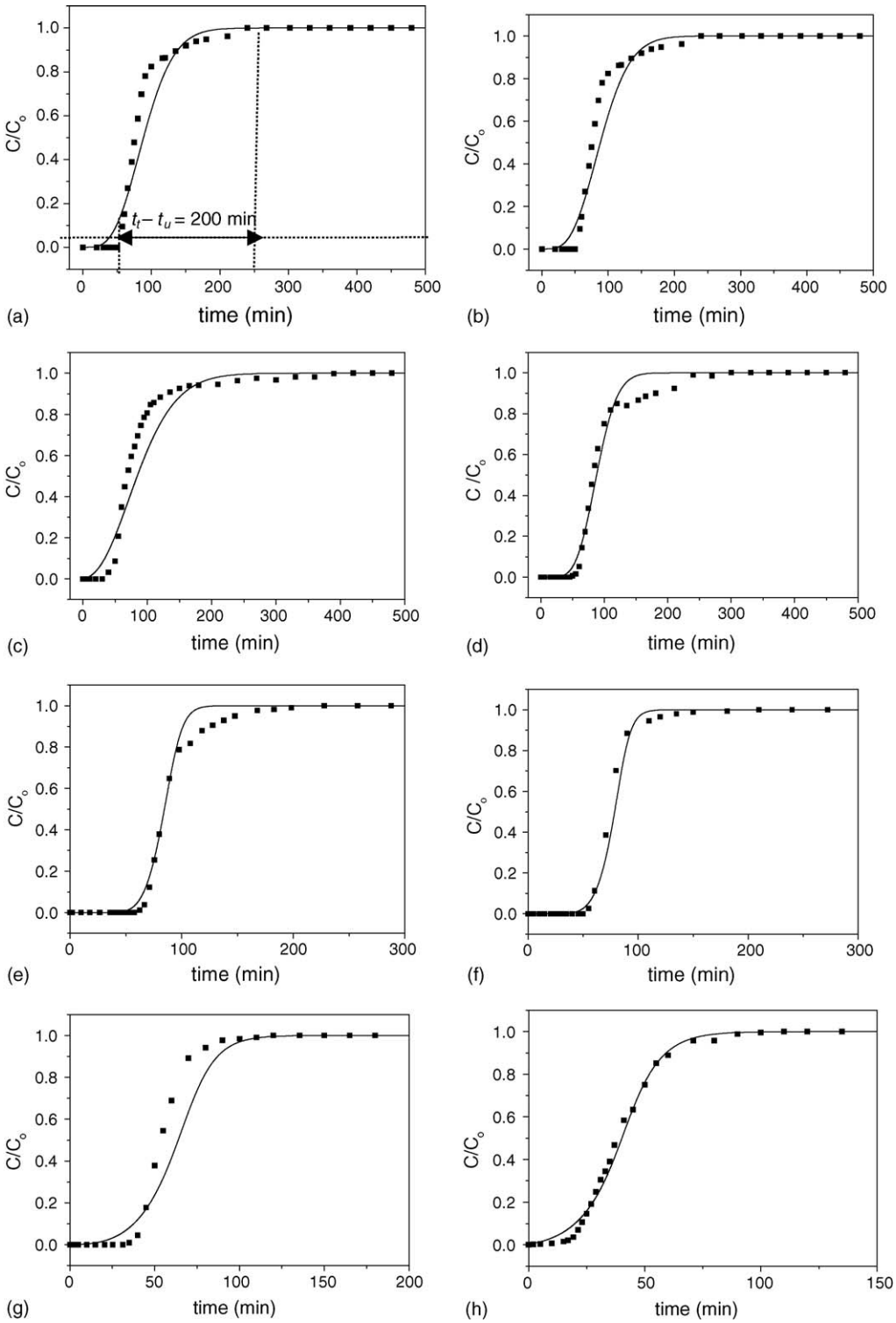

Fig. 2. Experimental breakthrough curve (■) and (—) simulated breakthrough curve of Cr–NaY with $H = 1.5$ cm: (a) $C_0 = 0.23$ mequiv./L; (b) $C_0 = 0.335$ mequiv./L; (c) $C_0 = 0.42$ mequiv./L; (d) $C_0 = 0.53$ mequiv./L; (e) $C_0 = 0.82$ mequiv./L; (f) $C_0 = 1.063$ mequiv./L; (g) $C_0 = 1.63$ mequiv./L; (h) $C_0 = 2.22$ mequiv./L.

procedure changed the partial equation system to an ordinary equation system. To solve the system of ordinary differential equations it was used the code DASSL [17]. This code solves systems of algebraic/differential equations and uses backward differentiation formulae to advance the solution from one time step to the next.

The axial dispersion coefficient (D_L) and the overall mass transfer coefficient in solid phase (K_S) were estimated using the

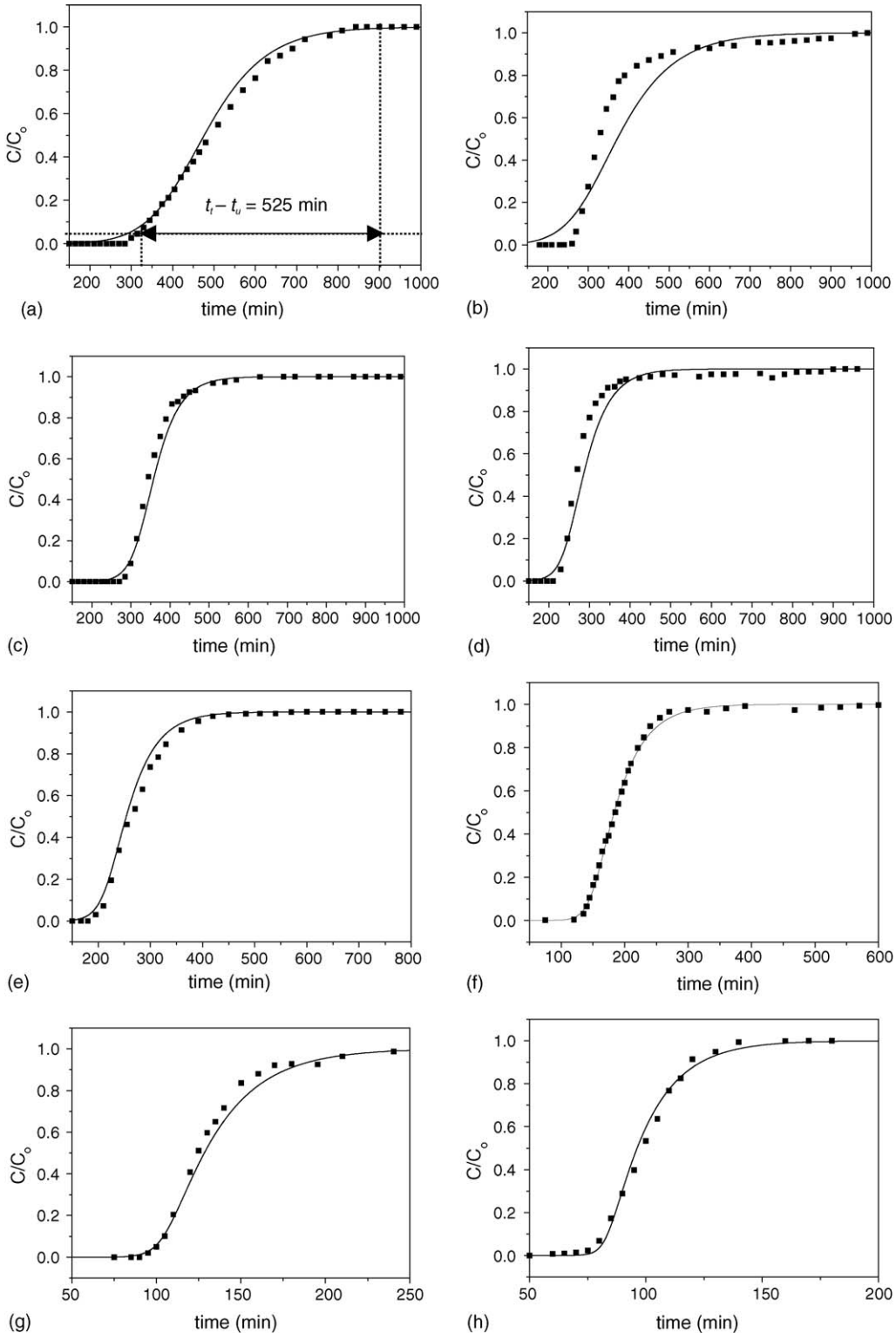

Fig. 3. Experimental breakthrough curve (■) and (—) simulated breakthrough curve of Cr–NaY with $H = 3.0$ cm: (a) $C_0 = 0.27$ mequiv./L; (b) $C_0 = 0.41$ mequiv./L; (c) $C_0 = 0.45$ mequiv./L; (d) $C_0 = 0.61$ mequiv./L; (e) $C_0 = 0.70$ mequiv./L; (f) $C_0 = 1.01$ mequiv./L; (g) $C_0 = 1.47$ mequiv./L; (h) $C_0 = 1.98$. mequiv./L.

experimental data of the breakthrough curves and the following objective function:

$$F = \sum_{i=1}^{np} (C_{out}^{EXP} - C_{out}^{MOD})^2 \quad (9)$$

where C_{out}^{EXP} is the experimental concentration of the Cr(III) in the outlet of the column, C_{out}^{MOD} the concentration of the Cr(III) determined by the solution of the model in the outlet of the column and np is the number of experimental data points.

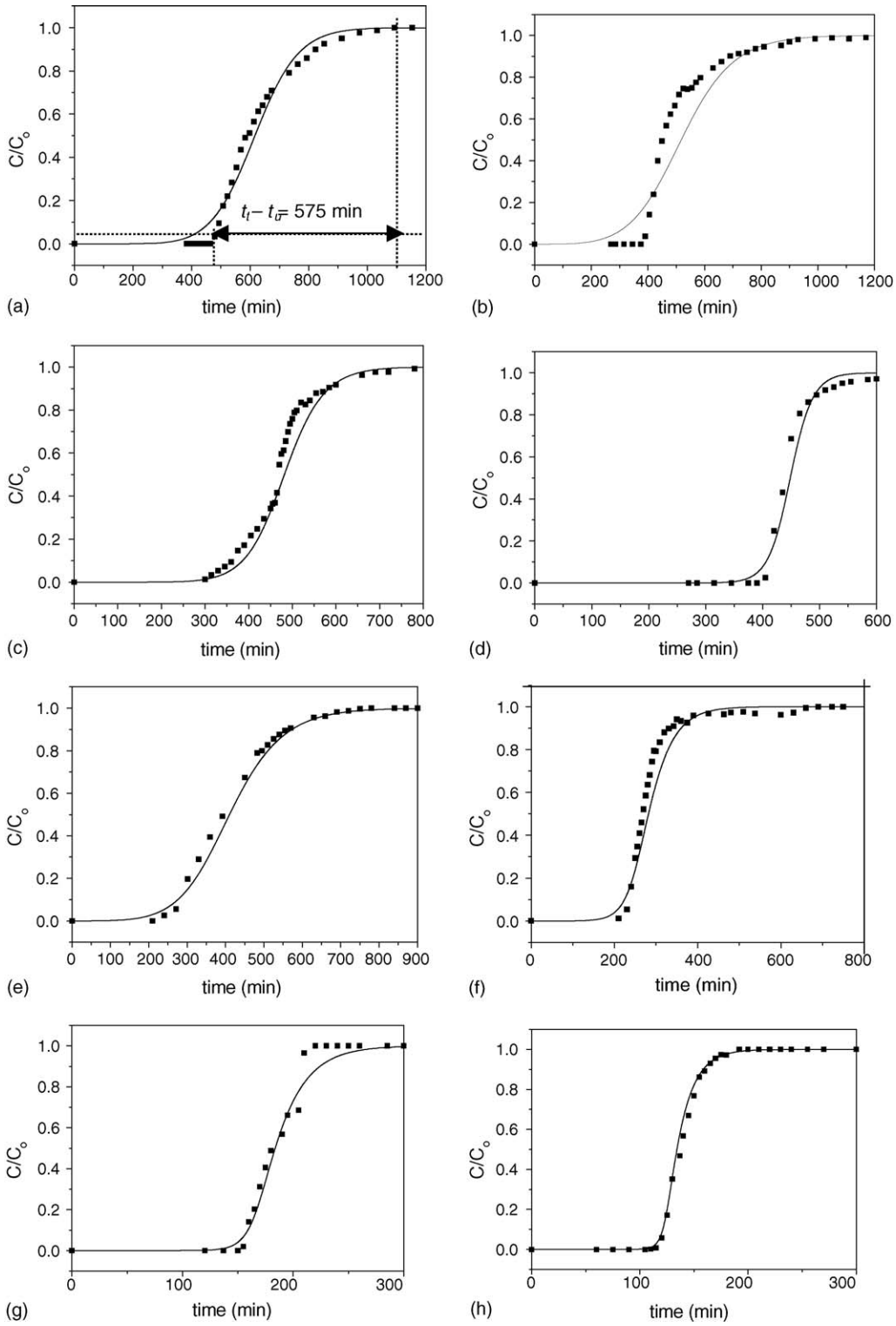

Fig. 4. Experimental breakthrough curve (■) and (—) simulated breakthrough curve of Cr–NaY with $H = 4.5$ cm: (a) $C_0 = 0.27$ mequiv./L; (b) $C_0 = 0.42$ mequiv./L; (c) $C_0 = 0.50$ mequiv./L; (d) $C_0 = 0.61$ mequiv./L; (e) $C_0 = 0.71$ mequiv./L; (f) $C_0 = 1.04$ mequiv./L; (g) $C_0 = 1.61$ mequiv./L; (h) $C_0 = 2.12$ mequiv./L.

3. Results and discussion

The breakthrough curves three beds heights generated the favorable dynamic isotherm shown in Fig. 1.

It was observed that the three isotherms tend to a plateau but with different values, close to 70% of the CEC that is 3.90 mequiv./g (2.73 mequiv./g), which means the occupation of the sites located in the large cages only [8]. For bed heights of 3.0 and 4.5 cm the experimental concentration of chromium in the zeolite ($q_{\text{max-exp}}$) is close to 2.8 mequiv./g while for 1.5 cm the value is lower at 2.5 mequiv./g. Therefore, it can be seen that the bed height influenced the dynamic equilibrium

mechanism. Probably such phenomenon is a consequence of chromium speciation [18] in the ion exchange process due to pH changes through the bed [19] and the internal resistance of the different species to diffuse through the micropores [14]. Then, differences in the equilibrium data were expected. In fact, the Redlich–Peterson model fitted different equations for each isotherm, as shown in Table 1.

Each equilibrium isotherm was used to fit the LDF model for breakthrough curves. As it can be seen in Figs. 2–4, such a model can successfully predict the experimental data if the internal resistance is considered as the rate controlling step. Therefore, such results are in total agreement with the hypothesis of diffusional problems faced by chromium ions through the microporous solid already discussed. Moreover, it is possible to observe different slopes for each breakthrough curve, even for those with similar concentrations and distinct bed heights. For example, for the more dilute concentration of approximately 0.27 mequiv./L, it was observed that the difference of the saturation time, where $C = C_0$ and the break point time, where $C = 0.05C_0$, $(t_t - t_u)$ is 200 min for the bed height of 1.5 cm (Fig. 2a) and similar values of 525 and 575 min for the bed heights of 3.0 (Fig. 3a) and 4.5 cm (Fig. 4a), respectively. Such results indicate, as would be expected from the equilibrium data, the influence of the bed height on the diffusion mechanism of chromium ions. In other words, these results indicate that the profile of the breakthrough curve varies with the bed height [20,21]. While chromium sorption occurs in the column, pH changes at each bed height Z. For the same running time t, the bed height Z has completely saturated zeolite sites, partially saturated zeolite sites or totally unsatured sodic sites [22]. At each value of Z, the pH is altered due to the presence of hydroxo-complexes in the cavities, changing, therefore, chromium speciation and as a consequence, the available amount of cation concentration for exchange. This provides a different ion exchange process at each bed height Z, which is more significant for the total bed height 1.5 cm when compared to 3.0 and 4.5 cm. Then, changes in the concentration of chromium in the zeolite can be explained by changes in the surface sorption properties during the binding of ions in the sites, which is more intensive at higher available cation concentrations [23] or in other words, lower bed capacity or smaller bed heights such as 1.5 cm. As a consequence, changes in the length of the mass transfer zone (MTZ) can occur. The hypothesis that it is constant and similar to the characteristic "S" shape profile is valid for ideal adsorption systems associated with adsorbates of small molecular diameter and simple structures [20], which was not the case investigated here.

In Fig. 5 the length of mass transfer zone (MTZ) was plotted against the feed concentration (C_0). In this figure one can observe that the bed height influenced MTZ as it was observed over a range of MTZ between 0.45 and 1.50 cm for $H = 3.0$–4.5 cm and a distinct one, between 0.30 and 0.80 cm for $H = 1.5$ cm. It probably happens because the rate at which the adsorption zone travels through the bed decreases with bed height [20]. Therefore, it may be concluded that the hypothesis of a constant length of mass transfer zone for the same feed concentration can be more acceptable depending on the variation of the bed height. The bed height of 3.0 cm is 200% the bed height of 1.5 cm. Then

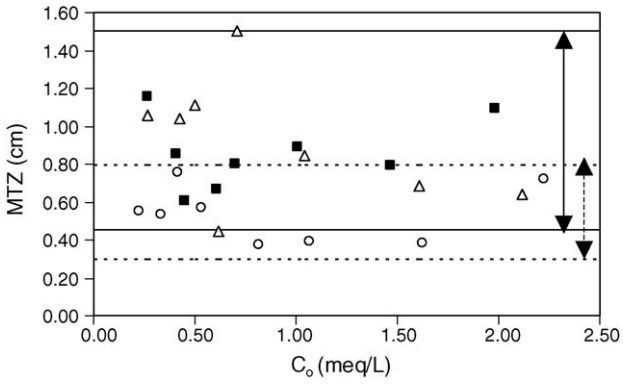

Fig. 5. Length of mass transfer zone (MTZ) for the breakthrough data: (◯) $H = 1.5$ cm; (■) $H = 3.0$ cm; (△) $H = 4.5$ cm; (—) range of mass transfer zone for $H = 3.0$–4.5 cm; (– – –) range of mass transfer zone for $H = 1.5$ cm.

it is reasonable to have differences in MTZ. On the other hand, the bed height of 4.5 cm is 150% the bed height of 3.0 cm. Then, in both cases the MTZ travels with closer rates.

The effect of bed height can be also seen in the overall mass transfer coefficient (K_S). In Fig. 6 one can observe distinct values of K_S, even for breakthrough curves obtained for the same feed concentration C_0. In fact, K_S values are similar to $H = 3.0$–4.5 cm and different to the values obtained for $H = 1.5$ cm, which is in total agreement with Fig. 5. The estimated model parameters are presented in Table 1. These results showed that K_S was changed with feed solution. Values of the overall mass transfer coefficient obtained through by Eq. (9) were related to the effective diffusivity of chemical specie in the solid [24].

As the rate at which the MTZ travels through the bed decreases with bed height, it was suggested that the pH changes and steric problems experienced by chromium species through the bed, provided more time to the Cr^{3+} ions to diffuse towards the exchange sites and higher K_S values for $H = 1.5$ cm where observed when compared to $H = 3.0$ and 4.5 cm.

It can be seen that the model predicts the overall mass transfer coefficient (K_S) and the axial dispersion coefficient (D_L). Therefore, it is wise to perform a sensitivity analysis to observe the overall effect of each parameter to the column system. It is presented in Fig. 7, where the sensitivity analysis was done for $H = 3.0$ cm and $C_0 = 1.983$ mequiv./L. The estimated values for K_S and D_L were 0.0593 min^{-1} and 1.92×10^{-2} cm^2/min, respectively.

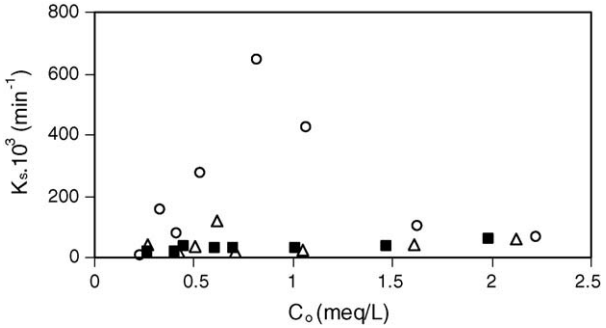

Fig. 6. Influence of bed height in the K_S values: (◯) $H = 1.5$ cm; (■) $H = 3.0$ cm; (△) $H = 4.5$ cm.

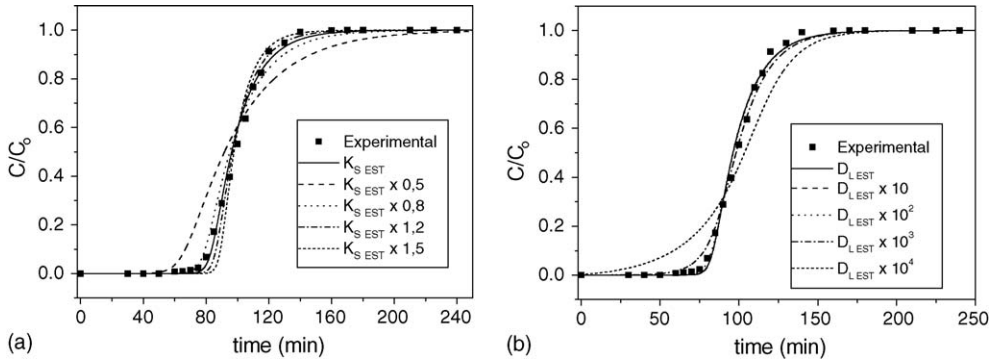

Fig. 7. Sensitivity analysis for the parameters: (a) K_S; (b) D_L.

It was found that K_S governed the slope of the breakthrough curves while D_L did not have a significant response even when this parameter varied up to $D_L \times 10^4$. Therefore, for each bed height, D_L can be assumed as an average of 8.25×10^{-2}, 1.04×10^{-2} and 3.36×10^{-2} cm^2/min for $H = 1.5$, 3.0 and 4.5 cm, respectively.

4. Conclusion

Chromium removal from aqueous solution by NaY zeolite was investigated in a fixed bed system. Mass balance equations were used to obtain the equilibrium isotherm in a dynamic process and equilibrium data provided a favorable isotherm fitted to Redlich–Peterson equation. It was concluded that the chromium ions occupy only the large cages of the zeolite and the equilibrium was bed-height dependent. The mathematical model used to represent the adsorption in the fixed bed column described well all the cases investigated. The mass transfer zone as well as the overall mass transfer coefficient also changed with different bed heights due to changes in pH through the column, which generated different chromium species. It was also concluded that changes in such parameters are a consequence of the velocity of the concentration profile through the bed. Therefore, for $H = 3.0$ and 4.5 cm, the velocity of MTZ through the bed can be considered almost the same, which generated similar K_S values. On the other hand, for $H = 1.5$ cm, the results showed a distinct behavior. The axial dispersion coefficient does not have a significant change for each bed column and may be considered as 8.25×10^2, 1.04×10^2 and 3.36×10^2 cm^2/min for $H = 1.5$, 3.0 and 4.5 cm, respectively.

Acknowledgments

The authors would like to thank Fundação Araucária for supporting this research.

References

[1] S. Kocaoba, G. Akcin, Removal and recovery of chromium and chromium speciation with MINTEQA2, Talanta (2002) 23–30.
[2] D. Bagchi, S.J. Stohs, B.W. Downs, M. Bagchi, H.G. Preuss, Cytotoxicity and oxidative mechanisms of different forms of chromium, Toxicology 180 (5) (2002) 22.
[3] M.A.S.D. Barros, P.A. Arroyo, P.A. García, E.F. Sousa-Aguiar, Environmental Problems and Catalytic Solutions. I. Chromium in the Tannery Industry, CYTED, Madrid, Spain, 2001 (in Spanish).
[4] S.I. Lyubchik, A.I. Lyubchik, O.L. Galushko, L.P. Tikhonova, J. Vital, I.M. Fonseca, S.B. Lyubchik, Kinetics and thermodynamics of the Cr(III) adsorption on the activated carbon from co-mingled wastes, Colloids Surf. A: Physicochem. Eng. Aspects 242 (2004) 151–158.
[5] R. Leyva-Ramos, L. Fuentes-Rubio, R.M. Guerrero-Coronado, J. Mendoza- Barron, Adsorption of trivalent chromium from aqueous solutions onto activated carbon, J. Chem. Technol. Biotechnol. 62 (1995) 64–67.
[6] L. Tagami, O.A.A. Santos, E.F. Sousa-Aguiar, P.A. Arroyo, M.A.S.D. Barros, NaY and CrY zeolites ion exchange thermodynamics, Acta Sci. 23 (6) (2001) 1351–1357.
[7] M.A.S.D. Barros, P.A. Arroyo, E.F. Sousa-Aguiar, C.R.G. Tavares, Thermodynamics of the exchange processes between K^+, Ca^{2+} and Cr^{3+} in zeolite NaA, Adsorption 10 (2004) 227–235.
[8] D.W. Breck, Zeolite Molecular Sieves, Robert E. Krieger Publishing Company, Malabar, FL, USA, 1974.
[9] M.A.S.D. Barros, A.S. Zola, E.F. Sousa-Aguiar, C.R.G. Tavares, Binary ion exchange of metal ions in Y and X zeolites, Braz. J. Chem. Eng. 20 (4) (2003) 413–421.
[10] F. Helferich, Ion Exchange, Dover Publications Inc., USA, 1995.
[11] C.J. Geankoplis, Transport Processes and Unit Operations, 4th ed., Pearson Education, USA, 2003.
[12] F.X. Stuart, D.T. Camp, Comparison of kinetic and diffusional models for packed bed adsorption, I & C Fundamentals 6 (1967) 156–158.
[13] Z. Zulfadhly, S. Mashitah, S. Bhatia, Heavy metals removal in fixed-bed column by the macro fungus *Pycnoporus sanguineus*, Environ. Pollut. 112 (2001) 463–470.
[14] M.A.S.D. Barros, I.F. Araújo Jr., P.A. Arroyo, E.F. Sousa-Aguiar, C.R.G. Tavares, Multicomponent ion exchange isotherms in NaX zeolite, LAAR (2003) 339–344.
[15] M.A.S.D. Barros, E.A. Silva, P.A. Arroyo, C.R.G. Tavares, R.M. Scneider, M. Suszek, Removal of Cr(III) in the fixed bed column and batch reactors using as adsorbent zeolite NaX, Chem. Eng. Sci. 59 (24) (2004) 5959–5966.
[16] T.-Y. Lee, T.-S. Lu, S.-H. Chen, K.-J. Chao, Lanthanum–NaY zeolite ion exchange. 2. Kinetics, Ind. Eng. Chem. Res. 29 (1990) 2024–2027.
[17] L.R. Petzold, A description of DASSL: a differential/algebric equation system solver, STR, SAND82-8637, Livermore, 1982.
[18] F.C. Richard, A.C.M. Bourg, Aqueous geochemistry of chromium: a review, Water Res. 25 (7) (1991) 807–816.
[19] A. Sánchez, A. Ballester, M.L. Blásquez, F. González, J. Muñoz, A. Hammaini, Biosorption of copper and zinc by *Cymodocea nodosa*, FEMS Microbiol. Rev. 23 (1999) 527–536.

[20] G.M. Walker, L.R. Weatherly, Adsorption of acid dyes on to granular activated carbon in fixed beds, Water Res. 31 (8) (1997) 2093–2101.
[21] J.-M. Chern, Y.-W. Chien, Adsorption of nitrophenol onto activated carbon: isotherms and breakthrough curves, Water Res. 36 (2002) 647–655.
[22] E.L. Cussler, Diffusion Mass Transfer in Fluid Systems, 2nd ed., Cambridge University Press, United Kingdom, 1997.
[23] S. Perić, M. Trgo, N. Vukojević Medvidović, Removal of zinc, copper and lead by natural zeolite—a comparison of adsorption isotherms, Water Res. 38 (2004) 1893–1899.
[24] F. Gleuckauf, J.I. Coates, Theory of chromatography, J. Chem. Soc. (1947) 1315.